Power curves of megawatt-scale battery storage technologies for frequency regulation and energy trading

Lucas Koltermann[a,b,c]*, Mauricio Celi Cortés[a,b,c], Jan Figgener[a,b,c], Sebastian Zurmühlen[a,b,c], Dirk Uwe Sauer[a,b,c,d]

[a] *Institute for Power Electronics and Electrical Drives (ISEA), RWTH Aachen University, 52074 Aachen, Germany*
[b] *Institute for Power Generation and Storage Systems (PGS), E.ON ERC, RWTH Aachen University, 52074 Aachen, Germany*
[c] *Jülich Aachen Research Alliance, JARA-Energy, 52056 Aachen / 52425 Jülich, Germany*
[d] *Forschungszentrum Jülich GmbH, Institute of Energy and Climate Research Helmholtz-Institute Münster: Ionics in Energy Storage (IEK-12), 52425 Jülich, Germany*

* Corresponding author. Tel.: +49 241 80 49338.
E-mail address: lucas.koltermann@isea.rwth-aachen.de

Abstract

Large-scale stationary battery energy storage systems (BESS) continue to increase in number and size. Most systems have been put into operation for grid services because of their technical capabilities. With increasing and more dynamic energy prices, their use in short-term energy trading such as day-ahead and intraday trading has also been gaining importance. In current technical and economic simulations and trading models, batteries are often used as an energy reservoir that can charge and discharge a constant power specified by the energy over a certain time. However, this simplification can lead to wrong results and makes economic assessments difficult. In order to successfully use BESS in energy trading, their real operating ranges and limits must be investigated, since batteries respectively BESS cannot deliver the same power over the entire state of charge (SOC) range. With a performance test of our hybrid BESS M5BAT, we show the characteristic performance curves for different battery technologies and consequently suitable operating ranges in a large-scale system configuration. The results show the wide range of challenges such as battery aging and balancing states that occur in the real-world implementation of BESS. The lithium-ion batteries of the system under test have a remaining usable energy between 75 % and 90 %, depending on the type of lithium-ion battery, while the usable energy of the lead acid batteries is only 60 %. The lithium-ion batteries were able to deliver a constant power output in the SOC range between 10 % and 80 %, which is a necessary requirement in short-term energy trading. The lead-acid batteries could only be discharged at full power in the range of 100 % to 50 % SOC and charged at full power between 0 % and 50 %. In the performance test, balancing was a limiting factor for lithium-ion batteries, while aging was the limiting factor for lead-acid batteries. Based on our findings, estimates for other existing BESS can be made to determine feasible operating ranges of these batteries for short-term energy trading. This also provides a guideline for individual tests that should be carried out on other BESS for verification.

Keywords: battery storage system power capability; cell variation; hybrid large-scale battery storage system; operation window; performance testing

Nomenclature

Abbreviation	Description
AC	Alternating current
BESS	Battery energy storage system
BMS	Battery management system
DC	Direct current
EMS	Energy management system
EPR	Energy-to-power ratio
FCR	Frequency containment reserve
LFP	Lithium-iron-phosphate
Li-ion	Lithium-ion
LMO	Lithium-manganese-oxide
LTO	Lithium-titanate-oxide
M5BAT	Modular Multi-Megawatt Medium Voltage Battery Storage System
NMC	Lithium-nickel-manganese-cobalt-oxide
OCSM	Lead-acid batteries with liquid electrolyte
OPzV	Sealed lead-acid batteries with gelled electrolyte
Pb	Lead-acid
SOC	State of charge
UTC	Coordinated universal time

1 Introduction

Energy storage systems are becoming increasingly important in the ongoing energy transition for the integration of renewable energies and grid stability [1–3]. Large-scale battery energy storage systems (BESS) in particular are benefiting from this development, as they can flexibly serve a variety of applications. Currently, BESS are already being used for grid services such as frequency containment reserve (FCR), the integration of large PV and wind parks, trading, energy and power optimization at industrial sites, and grid load management through grid boosters [4, 5].

While the use of BESS in grid services applications like FCR is widely adopted, the use of BESS in wholesale markets for energy arbitrage opportunities is not demonstrated that often. Wankmüller *et al.* [6] showed with their model the impact of battery degradation on energy arbitrage revenue potentials. Price arbitrage options in California and the actually observed battery activities were investigated by Lamp and Samano [7] and Zhang *et al.* [8]. But in [7] negative lifetime profits for BESS were named as concerns when used for energy arbitrage only. Further Investigations of energy arbitrage of energy storages in Texas were shown in [9]. All named studies on energy arbitrage have in common that they do not show tests or data of a BESS in field operation.

In current technical and economic simulations and trading models, batteries are often simulated as an energy reservoir that can charge and discharge a constant power specified by the energy over a certain time [10–12]. However, this is not how a real storage system operates. This simplification leads to wrong results and makes economic assessments difficult. It is therefore important to be able to take into account technology and system-specific features and characteristics [13].

Moreover, test and field data of large-scale BESS is not widely available. Calendar aging of BESS was investigated by Kubiak *et al.* [14] for a 250 kW/500 kWh system. Field test for frequency regulation services were performed with a 1.6 MW/400 kWh BESS by Swierczynski *et al.* [15]. The impact on a 1 MW system of different applications was investigated in [16]. A long-term study of a grid integrated BESS with 1 MW was examined in [17]. Extensive testing on batteries with reference to BESS was performed in several other studies [18–20]. A reference test for a Li-Ion BESS with 1 MW/250 kWh was performed by Dubarry *et al.* [21]. The results of the reference tests were used for tracking the efficiency and battery aging over time [21].

Digital twins for the detailed representation of large-scale BESS have already been developed and are currently being further developed. [22–24]. Reniers and Howey [22] show in their study a digital twin simulation for a 1 MWh grid battery storage. Modeling of cell capacity variation and degradation for use in simulations of BESS are presented in [24]. While Wu *et al.* [23] show the possibilities and perspectives of digital twins for BMS, it is

clear that real data are crucial for this development. Nevertheless, most studies are only simulations and lack validation with a real system.

Since field measurements to validate the digital twins are missing and energy arbitrage has not been demonstrated in the field so far, our aim with this study is to contribute filling this research gap. Energy arbitrage presents challenges for BESS due to the high power requirements, especially when considering the edge regions of the operating ranges of li-ion batteries in BESS. In this paper, we contribute with technology-specific power curves derived from a full field capacity test of a 7.5 MWh hybrid storage system available for public use. These measurements can be used to make digital twins as well as BESS models closer to reality and represent an additional value indispensable for their validation. Using the hybrid BESS M5BAT as an example, we present three lithium-ion and two lead-acid battery technologies to show how large-scale BESSs and the individual battery technologies behave under full load. The power curves derived can be used for the simulation of a BESS in all possible cases, ranging from grid-related studies to the integration of the power curves in ancillary service models and trading algorithms in industrial applications. Technical challenges within a BESS and the resulting limitations are highlighted. Concluding, we provide recommendations for the safe and reliable operation of BESS, specifically in the context of energy arbitrage, with the BESS M5BAT serving as an example.

2 Methodology

In this chapter the BESS M5BAT is described including the setup as well as the different battery units. The testing procedure performed with approximated timestamps is also outlined.

2.1 Battery storage M5BAT

The acronym M5BAT is short for “Modular Multi-Megawatt Medium Voltage Battery Storage System” and is a BESS with ten independent battery units with five different battery chemistries. In sum M5BAT has a nominal energy of 7.5 MWh and a nominal power rating of close to 6 MW. The BESS M5BAT is in operation since 2017 and due to aging and for battery protection only 5.3 MW are actively used. In Table 1 the battery units with the nominal energy and power ratings are listed. Also, the average C-rates for the year 2022 and the measured efficiencies for each battery unit are outlined. In past studies, various areas of the BESS M5BAT have already been explored, such as the influence of FCR on BESS [25–27], operating strategies [28–30], and BESS response times [31].

Table 1: Technical battery description of the battery units and technologies of M5BAT. Note: The LFP battery unit has a larger energy content according to the type label (in brackets) than according to the technical description. [25–27, 32, 33]; the shown C-rate takes only data points with an absolute current larger than 0.01 C into account.

Battery unit	Technology	Abbreviation	Nominal energy at 1/3C in kWh	Nominal energy at 1C in kWh	Power limit in kW	wiring	measured kWh efficiency in % in 2022	measured Ah efficiency in % in 2022	Measured average absolute C-rate in 2022
1	OCSM	Pb1	1066	749	450	300s1p	83.98	96.88	0.1521
2	OCSM	Pb2	1066	749	450	299s1p	86.63	99.20	0.1586
3	OPzV	Pb3	843	602	315	308s2p	81.88	93.66	0.1452
4	OPzV	Pb4	740	504	315	306s1p	81.93	96.53	0.1618
5	LMO/NMC	LMO1	774	724	630	192s16p	97.82	99.11	0.2374
6	LMO/NMC	LMO2	774	724	630	192s16p	97.93	98.22	0.2368
7	LMO/NMC	LMO3	774	724	630	192s16p	98.06	98.35	0.2368
8	LMO/NMC	LMO4	774	724	630	192s16p	97.79	99.08	0.2401
9	LFP	LFP	738 (923)	708 (886)	630	240s10p	96.36	99.00	0.2323
10	LTO	LTO	> 230	230	630	312s32p	95.95	100.25	0.5312

The connection scheme as well as the battery availability of M5BAT can be found in [27]. For this study all ten battery units were active and in operation. Due to aging most battery units cannot deliver the nominal energy. In addition, especially with lithium-ion battery units, voltage differences between the individual cells are relevant. These limit the usable energy

and capacity. However, the unusable areas can be kept low by suitable balancing procedures.

2.2 Testing procedure

The testing procedure is designed in a simple way, which puts a heavy load on the battery units and gives insights into the remaining performance of the BESS, but requires planning. For the test, all ten battery units are active and the whole BESS participates in the intraday energy market to buy energy for charging and to sell energy for discharging. Thus, a discharge/charge cycle is performed through the power provision of the BESS on the energy market. A technical flowchart of the testing procedure is illustrated in Figure 1.

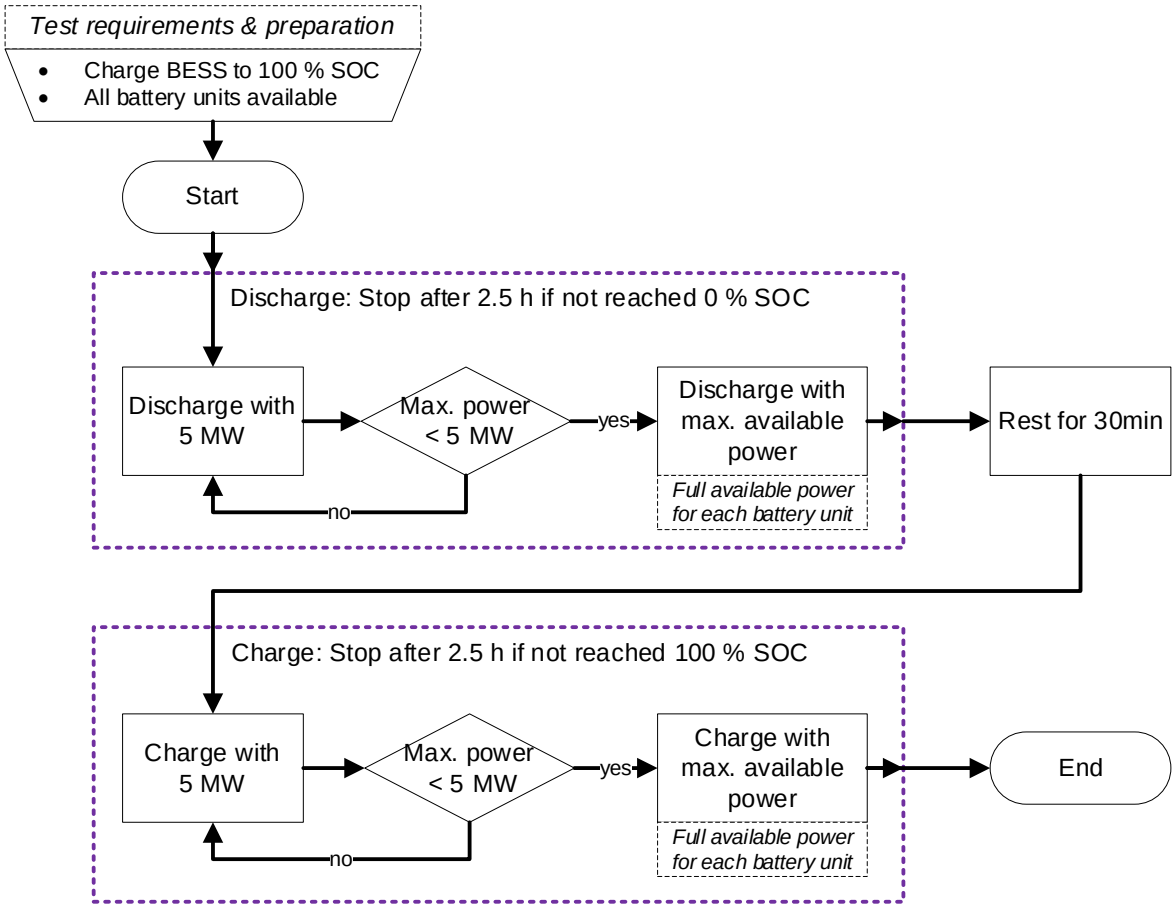

Figure 1: Technical flowchart of the testing procedure

Before the test starts, the BESS is charged as close to 100 % as possible and it is ensured that all battery units are available. The maximum power in charging and discharging direction is limited to 5 MW or the largest possible power output of the BESS if this value is smaller. If the power drops below 5 MW, this indicates that all battery units are delivering the maximum available power, while at a power of 5 MW, the power distribution algorithm dynamically distributes the power among the battery units [33]. Since hourly, half-hourly, and quarter-hourly products are traded in the intraday and day-ahead markets, high charging and

discharging rates are particularly relevant. The test duration is thus limited to 2.5 h per power flow direction, as very low power flows are expected for even longer test durations and the testing time for the BESS M5BAT is limited due to operational reasons. If some battery units are not fully charged or discharged after 2.5 h, the test is finished for these battery units, as the remaining low power can only be marketed to a very limited extent and therefore does not play a decisive role. In Table 2 the approximate timestamps and observed actions are listed.

Table 2: Testing procedure with approximate time and performed actions. The battery units were charged and discharged as long as the BMS allowed it. The comment completely charged and completely discharged refers to the maximum allowable charge or discharge by the BMS.

Approximate time (UTC)	**Action / Comment**
9:00	Test starts – discharging with 5 MW
9:30	LTO battery completely discharged
10:00	LFP battery completely discharged
10:15	All Li-Ion batteries completely discharged
11:40	Test discharging stopped. Discharging for Pb-battery units stopped.
12:00	Test starts – charging with 5 MW
12:45	LTO battery completely charged
12:55	LFP battery completely charged – Balancing starts
13:30	All Li-Ion batteries completely charged
14:30	Test charging stopped. Charging for Pb-battery units stopped.

Due to the time limitation of the test, it is possible that not all batteries will be fully charged or discharged. For this reason, there will be edge areas that are not covered by the test and for which statements can only be made on the basis of operational experience.

3 Results and discussion

The results are divided into system-wide results for the whole M5BAT BESS to cover the grid perspective and individual results for each battery unit. Note that a positive power or current value always corresponds to discharging the battery units or the BESS while a negative power or current value means charging the battery units or the BESS.

3.1 Grid perspective – BESS M5BAT

In this section results for the whole BESS M5BAT and measurements at the grid connection point are shown. These results are especially for front-of-meter applications like energy trading and grid services relevant. Due to the special characteristics of BESS the limits of the "energy reservoir" concept are pointed out. It is explained why, with sufficient nominal energy, not all energy products can be equally served.

In order to better understand the test procedure, Figure 2 shows the power curve according to Table 2. The test started with discharging the BESS at 5 MW. After approximately 30 min the graph in Figure 2 shows a decline to 4.5 MW. At this point in time the LTO battery unit was nearly completely discharged, which resulted in the reduction of its power output. The LTO battery has a lower energy-to-power ratio (EPR) than all other battery units and reaches full charge or full discharge state at equal power output faster than the other battery units (Table 1). Thus, from that point onwards, the maximum power output is lower than 5 MW. The next prominent point is around 10:00., where an exponential drop-off in the power output is visible. Around that time, the other lithium-ion battery units (LMO and LFP) entered the constant voltage phase so that the power output was drastically reduced. From there on, only the lead-acid battery units had energy available to discharge, while the power output constantly became smaller until the test was stopped.

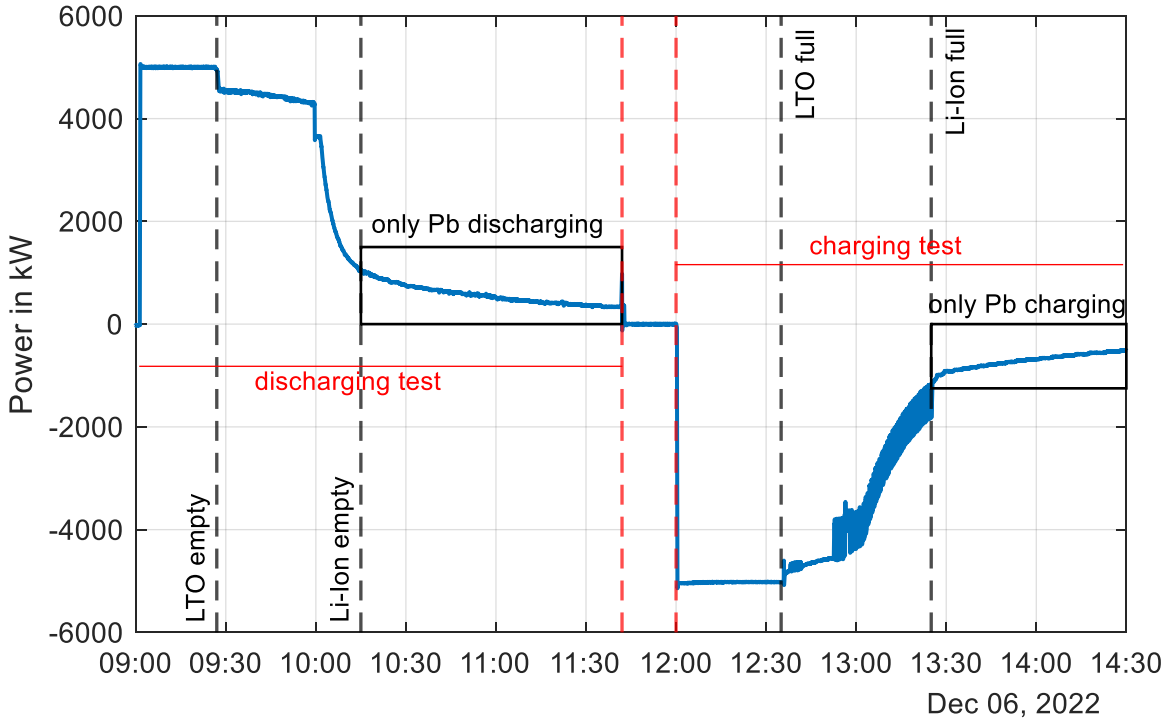

Figure 2: Power over time for the entire test process with approximate time entries timestamps for relevant events.

After a short pause, the charge process was started around 12:00 (Figure 2). For the entire charging process, an inverted pattern is apparent. At first, the LTO battery unit became fully charged followed by all other lithium-ion battery units. In contrast to the discharging process, the constant voltage phase and the following power reduction start earlier during charging and can be continued at a reduced level for longer until a full charge is achieved. After the full charge of all lithium-ion battery units, only the lead-acid battery units charge further. Again, the charging power of those battery units constantly decreases until the end of the test.

Figure 3 shows the state of charge (SOC) for the BESS M5BAT over the testing time and the cumulated charged and discharged energy. The SOC for the BESS M5BAT (SOC_{M5BAT}) is the capacity weighted average value of all individual battery units and is calculated according to equation (1). The index i represents the battery unit according to Table 1 while battery units' SOC value is named ($SOC_{battery}$). The batteries SOCs are weighted by their nominal capacity ($C_{nom_{battery}}(i)$) in relation to the sum of all battery unit's nominal capacity.

$$SOC_{M5BAT} = \sum_{i=1}^{10} \left(SOC_{battery}(i) \bullet \frac{C_{nom_{battery}}(i)}{\sum_{i=1}^{10} \left(C_{nom_{battery}}(i) \right)} \right) \quad (1)$$

At the steep sections of the SOC-line the charged or discharged energy increases at a high rate. As expected, the change in the energy at the flat areas of the SOC curve is correspondingly small.

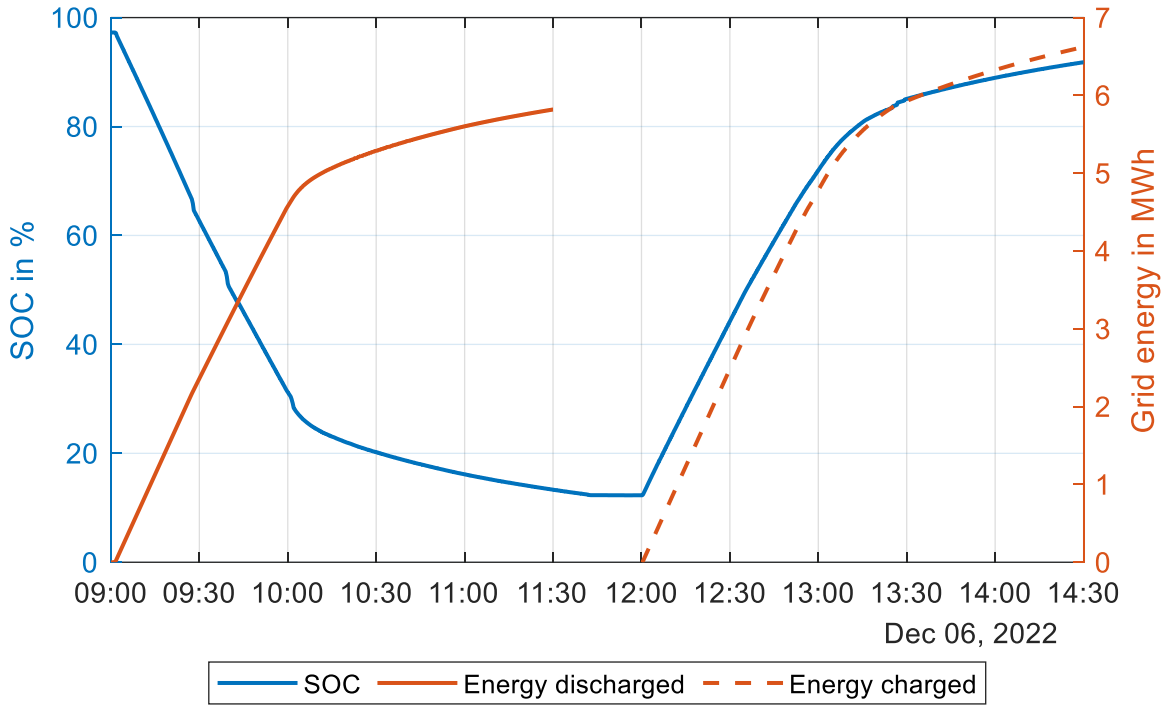

Figure 3: M5BAT SOC and cumulated charged and discharged energy at the network node

In total, more energy is charged than discharged due to energy losses in power electronics, transformers and batteries. However, it is worth noting that more SOC percentage points were discharged than charged, and that the SOC value at the end of the test is lower than at the beginning of the test. This unexpected behavior has multiple reasons. The energy shown is measured at the grid node or connection point, where front-of-the-meter applications have to deliver power. Between the battery units and the grid node there are inverters and transformers necessary to convert the power from DC to AC and achieve the desired voltage level, respectively. These conversion steps cause losses which result in less energy from the battery units reaching the grid node while discharging. For the charging process the BESS needs to draw more energy from the grid than the BESS can store in the battery units. In addition to the conversion losses, multiple battery units perform balancing actions when fully charged. This process needs additional energy and makes more energy content available for the user. This balancing process can also lead to a discrepancy between charging and discharging energy.

In Table 3 the energy charged and discharged for the entire test (2.5 h) and for 1 h is listed. For 1 h the charged energy is only 200 kWh higher than the discharged energy. The 2.5 h values for the entire test show a discrepancy of around 800 kWh.

Table 3: Charged and discharged energy for the BESS M5BAT

Time	**2.5 hours**	**1 hour**
Charged AC energy in MWh	6.62	4.78
Discharged AC energy in MWh	5.81	4.58

Finally, the measured performance curves for the BESS M5BAT are presented in Figure 4. Due to the test limit of 5 MW per power flow direction, the measured power curves also reach only this maximum despite the battery units could in total deliver up to 5.2 MW. The SOC ranges between 0 % and 12 % as well as 95 % to 100 % are not shown in Figure 4 because the measurement was not performed in that range. Due to time constraints for the testing session the test is limited to 2.5 h for charging and discharging. The lead-acid batteries could not be charged or discharged completely within the time limit, which led to the SOC ranges named before. We assume that for discharging the full power of 5 MW could also be delivered in the upper 5 % SOC and full charging power of 5 MW could also be delivered in the lower 12 % SOC range. Since only the lead-acid batteries are responsible for the missing SOC ranges, the assumption is based on BMS knowledge of the lead-acid batteries, which allow charging and discharging performance based on the SOC. Thus, the discharge power in the highest SOC range and the charge power in the lowest SOC range increases and the assumed 5MW discharge and charge power can safely be provided.

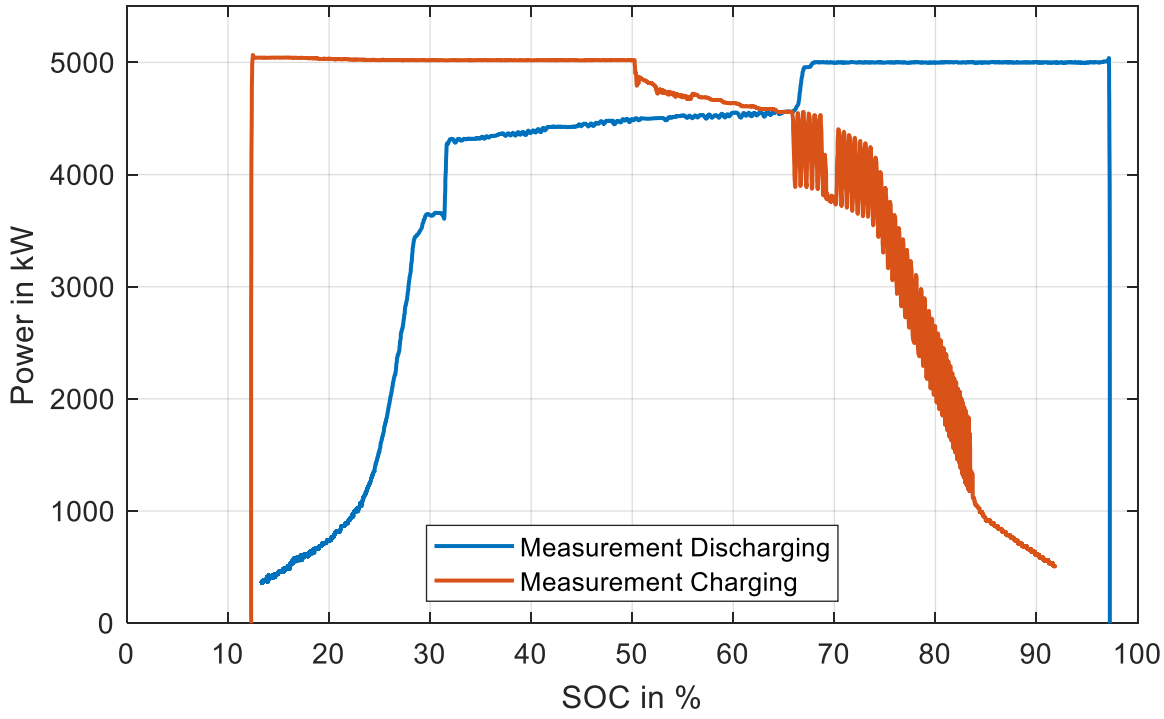

Figure 4: Charging and discharging capability over SOC for the M5BAT BESS. Note: The shown curve is plotted of a weighted SOC but the battery units were at different SOC levels.

Since the battery units had different SOCs in the measurement and only correspond to the SOC shown in the totality, the already discussed distinctive points and areas result in the measurement curves. The measurements thus show charge and discharge performance under constant full load. The power curves for the individual battery units are presented in section 3.2 “Battery perspective”.

If BESS are considered as energy reservoir, as an example of M5BAT with a nominal energy of about 7.5MWh, it could be expected that 5MW can be provided over 1h and thus marketed in the intraday market as 1h product. As the power curves show, this amount of energy is in principle available, but only at lower charging or discharging rates. Moreover, at low (<10%) or high charge rates (>90%), only very limited power can be discharged or charged, so that these charge rates should be avoided in regular operation. At states of charge <20% or >80%, a strong throttling of the power outputs is already clear, so that attention must be paid to the battery-specific properties when marketing in this range.

Depending on the battery technology, this results in an individually usable operating window for full power or for reduced power. Section 3.3 shows the operating windows determined using the example of M5BAT.

3.2 Battery perspective

In this section the battery units are investigated and technology specific power curves are generated. Moreover, for the li-ion battery units the cell balancing is examined and compared to each other. The results show the technology specific capabilities which can be useful when looking for a BESS if a use case is predetermined.

The battery units’ section is divided in three parts, tackling the power and SOC curves at first. Then the results for observed mean cell voltages and cell currents are presented. Following, the charged and discharged energy per battery is shown and the usable energy in relation to the nominal energy is evaluated. The data shown is unique in that it comes from a real BESS that has been in operation for nearly 6 years and allows the direct comparison of different technologies at comparable loads.

3.2.1 Battery units: Power and SOC curves

The power curves for each battery unit for the test is presented in Figure 5 for the DC-side of the inverters. The LTO battery unit which is only active for the first half hour in the discharging and charging test, shows frequently changing power outputs around 300 kW to 400 kW. The LTO battery unit is capable of delivering the full 630 kW, but in the test only 5 MW of the available 5.2 MW for the BESS were requested and the power distribution algorithm chose to request from the LTO battery unit only around 400 kW of the available 630 kW [33]. All other battery units started with delivering their maximum available power

output. The power limitation for each battery unit can be found in Table 1. Due to a similar energy content, all lithium-ion battery units reached a comparable power output. Notably at the lead-acid battery units is that shortly after starting the test the Pb 1 unit reduced the power output compared to the Pb 2 unit despite those units are identical in design. The lower power capability of the Pb 1 unit could be a reason of further progressed aging or a poor SOC calculation of the battery management system (BMS) by the manufacturer. A similar behavior of the lead-acid battery units is visible in charging direction at around 12:30. During the charging process, the LFP battery unit is clearly noticeable due to extreme fluctuations in the power input after about one hour in the test. These fluctuations indicate an almost 100 % SOC. Due to a poor BMS implementation by the manufacturer, this can be the beginning of the balancing process. All other smaller fluctuations in the power curves came from controlling the power output near the targeted 5 MW and the control algorithm as well as from BMS corrections and making more or less energy available to charge or discharge.

Due to the power setpoints refer to the inverters AC-side the power values on DC-side are higher for discharging and lower for charging. This difference is created by the inverter losses. From the DC-power values in Figure 5 the E-rates of the battery units are calculated and also shown in Figure 5. The E-rate is defined in equation (2). $P_{DC_{Batt}}$ indicates the DC-power of the battery unit while $E_{nom_{Batt}}$ marks the nominal energy per battery unit.

$$E\text{-}rate = \frac{P_{DC_{Batt}}}{E_{nom_{Batt}}} \tag{2}$$

The E-rate for the LTO battery unit is with values up to 2 E and -2.3 E a lot higher than the E-rates for all other battery units. Due to the low nominal energy of the LTO battery unit but an equal high power capability, the stress through the E-rates is higher for the LTO battery unit. The EPR for the other battery units makes E-rates over 1 for the other battery units impossible.

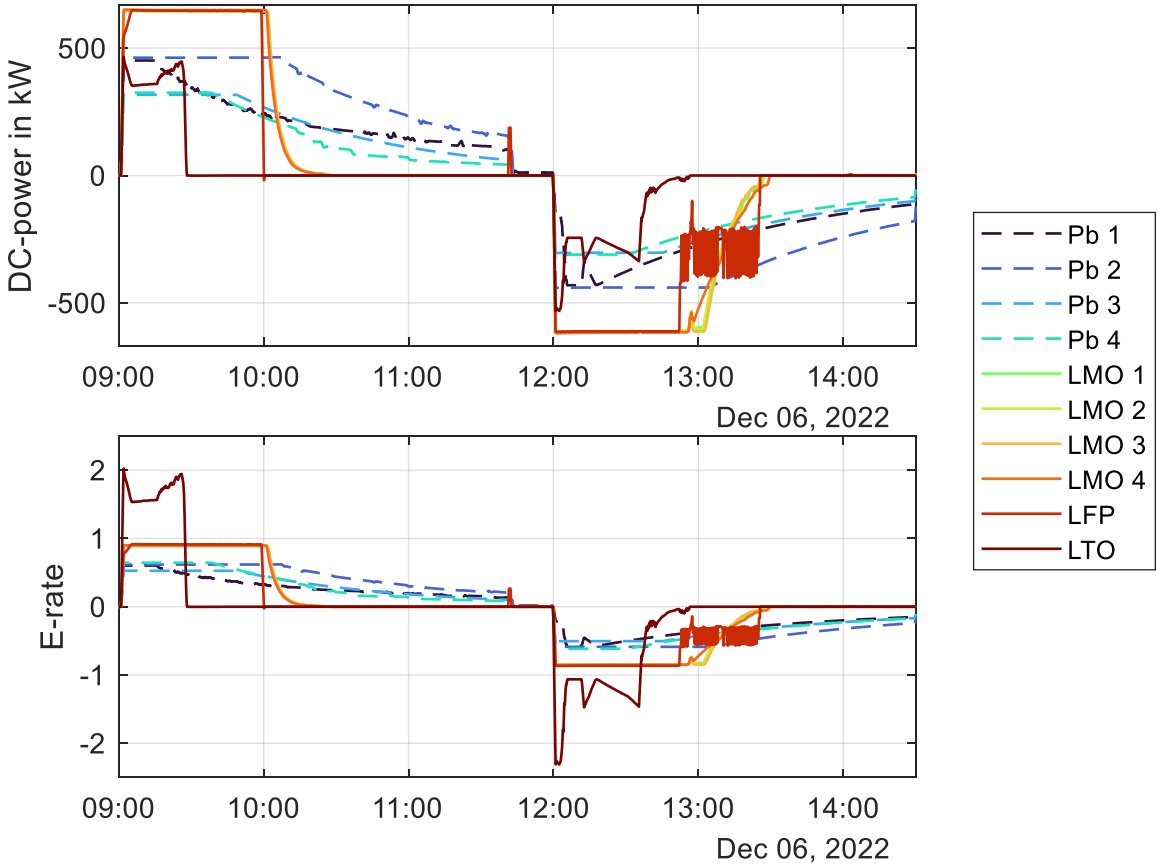

Figure 5: Power curve on inverters DC-side per battery unit and corresponding E-rate for the battery units. Note that for the LTO battery unit not the full power available was requested.

Next to the power output, the SOC curves, which are corrected by the SOH detected by the BMS are shown in Figure 6. The dotted SOC line represents the entire BESS and is already shown in Figure 3. The LTO SOC curve is compared to all other SOC curves a lot steeper. Since the LTO battery unit has experienced higher E-rates, this corresponds to a higher charge/discharge rate and faster SOC changes compared to the other battery units.

A jump from 0 % to approximately 10 % SOC is also visible in the curve of the LTO battery unit. This jump is a SOC correction of the BMS. Due to low cell voltages of the battery unit and large spreads, the battery unit was not discharged further for protection. The LFP battery unit was also not discharged to below 8 % SOC to protect the battery. The charging and discharging curves of all lead-acid battery units are compared to the lithium-ion battery units a lot flatter. Due to low charging and discharging power but high nominal energy the available and observed charging rates are relatively low.

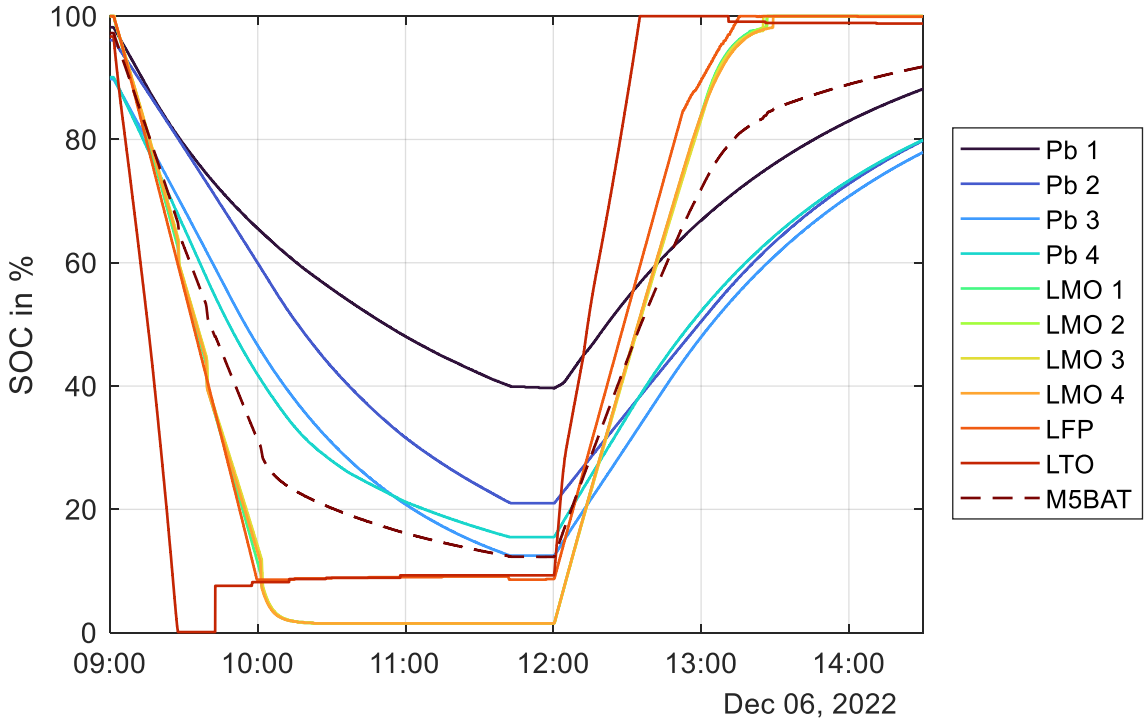

Figure 6: SOC curve for each battery unit and the dotted line for the entire BESS M5BAT

For high power applications lithium-ion batteries a better suited than lead-acid batteries. The dents and jumps in the SOC curves as well as the dents in the power curves before indicate that a well implemented BMS and regular maintenance and balancing processes are absolutely necessary to operate a large-scale BESS to keep those discontinuities as small as possible.

3.2.2 Battery units: Cell voltages and currents

The characteristics of different battery technologies become clear when looking at the voltage curves of the cell voltages in Figure 7. The overall voltage level is directly dependent on the technology respectively on the material used in the battery cells. Independent of the battery chemistry a higher cell voltage corresponds to a higher SOC while a lower cell voltage corresponds to a lower SOC. Further, there are overpotentials in the charging and discharging process which will not be discussed in this study but can be found [34, 35]. The highest voltages can be observed for the LMO battery units with voltages between 3.4 V and 4.1 V. The LFP battery unit shows cell voltages between 3 V and 3.4 V while the LTO battery cell voltage lies between 1.9 V and 2.8 V in operation. The voltages for all lead-acid batteries are lower and can be found between 1.8 V and 2 V for the discharging process and between 2.1 V and 2.4 V for the charging process.

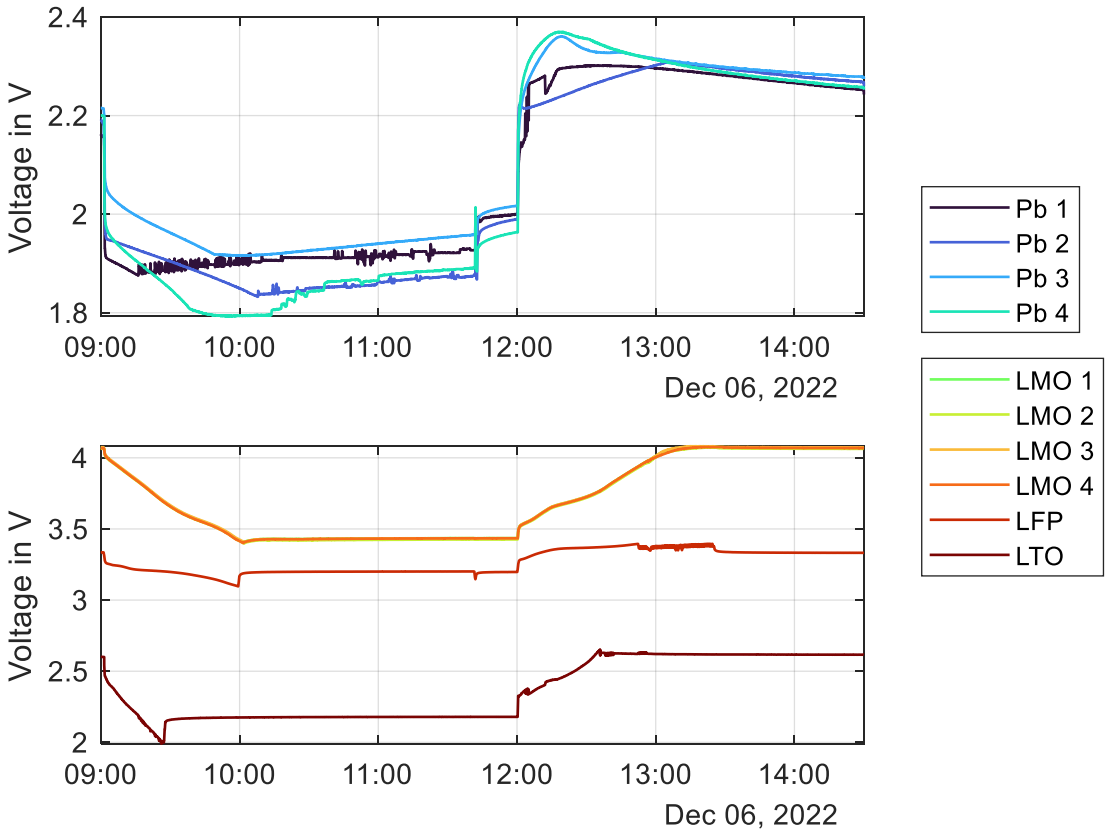

Figure 7: Mean cell voltage per battery unit

Next to the mean cell voltages, the mean cell currents are presented in Figure 8. Since the wiring of the individual cells varies between the battery units, the average cell currents are also very different. The wiring is introduced in Table 1. Generally, li-ion batteries are connected by multiple parallel cells while lead-acid batteries are connected mostly only in series. The parallel structure of the li-ion battery units leads to lower cell currents compared to lead-acid batteries.

The discharging and charging process in this test started with a constant power phase, which corresponds to steadily increasing currents in the discharging process and steadily decreasing currents in the charging process. This behavior can be seen in Figure 8 and is valid for all battery units which performed a constant power phase.

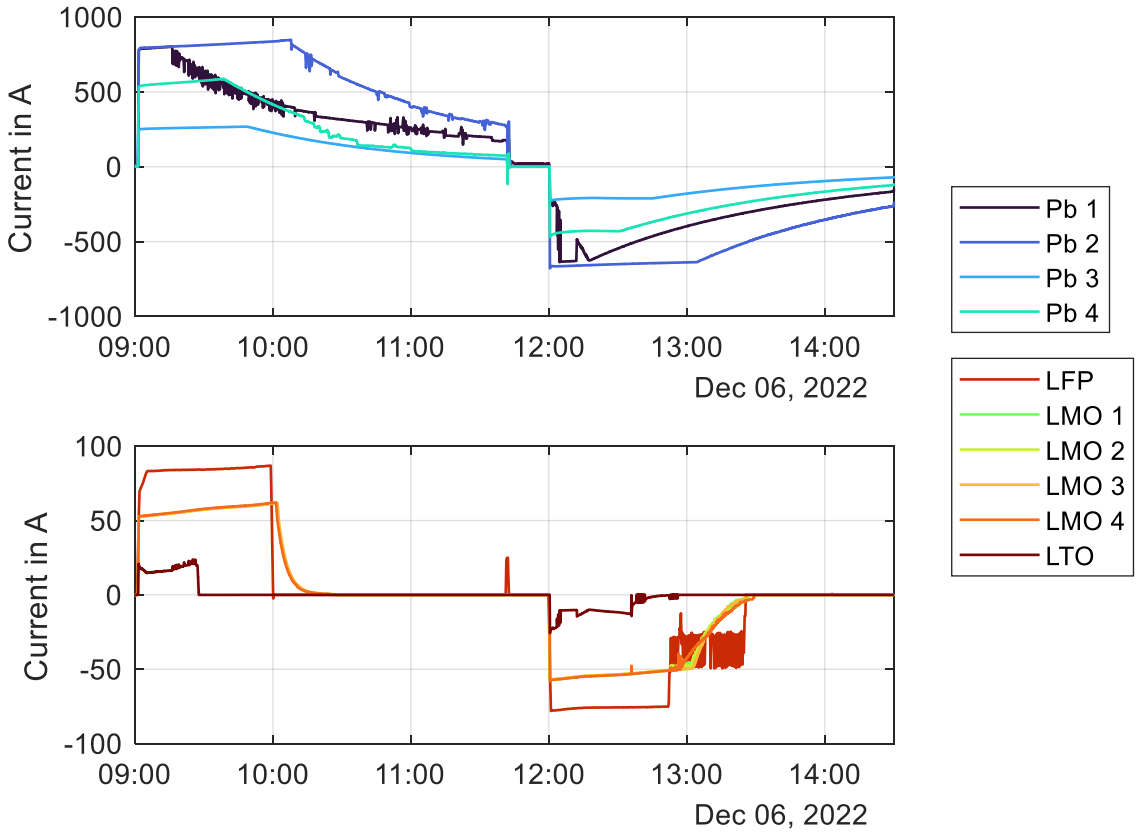

Figure 8: Mean cell current per battery unit

3.2.3 Battery units: Power and energy

Especially important for marketing activities is the knowledge over the technology dependent power capabilities over the different battery technologies. In Figure 9 the characteristic performance curves for discharging and charging for all ten battery units are shown. In Figure 9 the curves do not reach 0 % SOC for charging or 100 % for discharging because these SOC levels were not used in the testing procedure. Due to a lower power allocation to the LTO battery unit, the curves for the LTO battery are not generally valid. The power capability of the LTO battery unit is similar to all other lithium-ion batteries tested and only limited by the inverters power capability.

The ripples on the curves in Figure 9 occur for two different reasons. The testing refers to a 5 MW output of the entire BESS and to reach this value at the grid connection point a PI-controller is implemented. Measurement uncertainties as well as controller delays and reaction times cause an output power which hovers around 5 MW and causes ripples in some curves. For the lead-acid battery a two-point controller implemented within the BMS can also cause ripples. The BMS monitors all cell voltages and if a too low cell voltage is detected the overall power output is reduced. The controller tries to reach the maximum available

power based on the cell voltage. Due to an insufficient adaption to the aging of the battery, the two-point controller protects the battery cells against damages but induces ripples in the maximum power output. The ripples of the LFP battery unit in the charging test are caused by a balancing process and discussed in section 3.2.5.

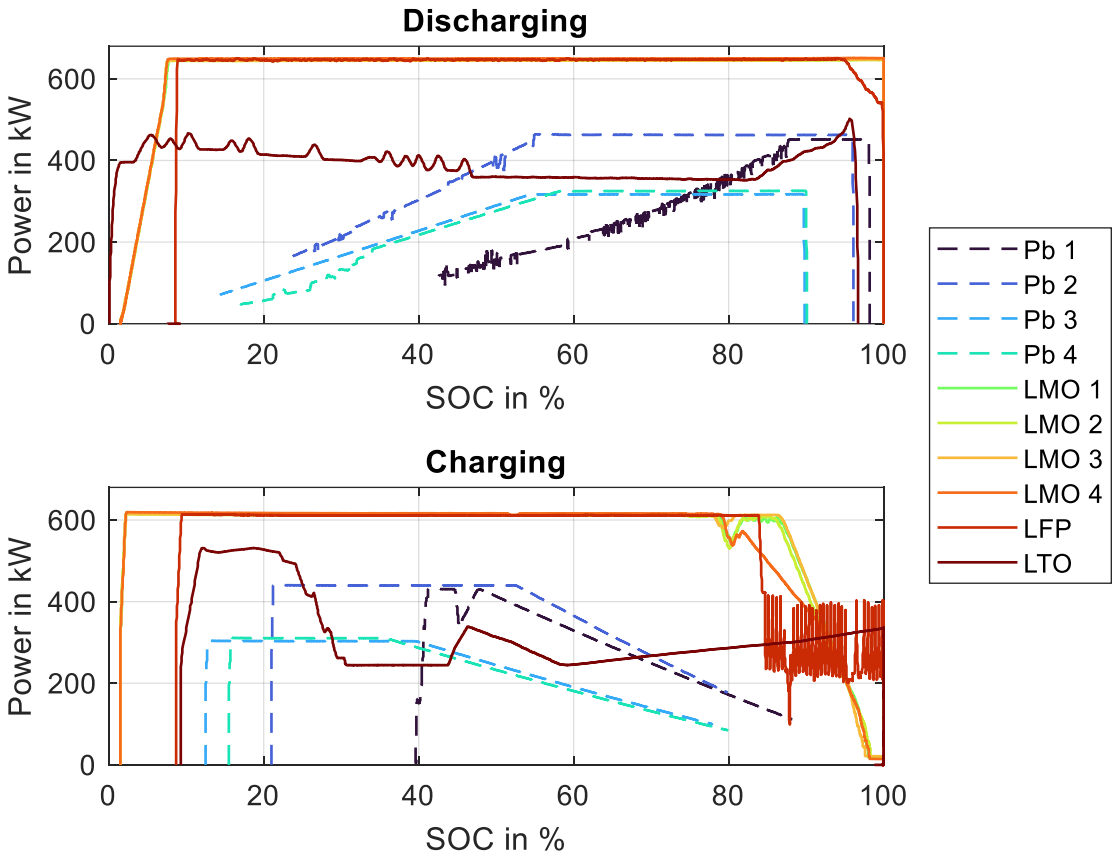

Figure 9: DC power output for each battery unit vs. SOC level

As a rough summary of battery usage, it can be stated for lead-acid batteries that from 100 % to approximately 50 % lead-acid batteries can be discharged at full power. After that, the power must be throttled to protect the battery. For the charging process, a similar limit applies up to approximately 40-50 % SOC can be charged with full charging power. At the latest from 55 % onwards, the charging power must be reduced.

In contrast, for lithium-ion batteries, it is shown that reduction of the discharge power is only necessary from about 10 % SOC. The reduction then follows an exponential curve. For the charging process, it is shown that charging can be carried out at full charging power up to around 80 %, from where a linear to exponential curve becomes apparent. Lithium-ion batteries can thus be charged and discharged at full power in wide ranges of the SOC.

In Figure 10 the usable energy is shown for all battery units with distinction to a 1 h value and a 2.5 h value. For the lead-acid battery units both the 2.5 h value and the 1 h value uses 1/3 C-rate nominal energy from Table 1 because those battery units were loaded with a C-

Rate in that range. The li-ion battery units' usable energy is calculated for both values with the nominal energy from Table 1 at the 1 C-rate. For the lead-acid batteries the 2.5 h usable energy value is mostly a lot higher than the 1 h value. This could indicate that by battery aging the lead-acid batteries are not capable of providing high charge or discharge power outputs anymore. For the lithium-ion batteries, the difference between those values is very low or non-existent. Looking at the LTO battery unit, the values are identical because the LTO battery unit was discharges in less time than 1 h and has no significant difference in energy for different C-rates. The usable energy value of around 70 % for the LTO battery unit in Figure 10 shows off the effect of bad balancing. The estimated SOH lies at around 95 % so the balancing makes 25 % of the nominal energy unusable. With the LFP battery unit, about 85 % of the capacity can be used with a battery aging of less than 5 %. So here, about 10 to 15 % of the nominal energy cannot be used due to the lack of proper balancing. It is noticeable on the LFP battery unit that the 1 h value of the usable capacity is greater than the 2.5 h value. This is due to a discharge duration of just under 1 h. A longer discharge duration was expected and more energy could be discharged at slightly lower c-rates.

All LMO battery units show a similar picture, of 90 % usable energy. The value for 2.5 h is slightly higher because the discharge time was longer than 1 h and the low discharge rate at the end of the discharge process is only taken into account for the 2.5 h value.

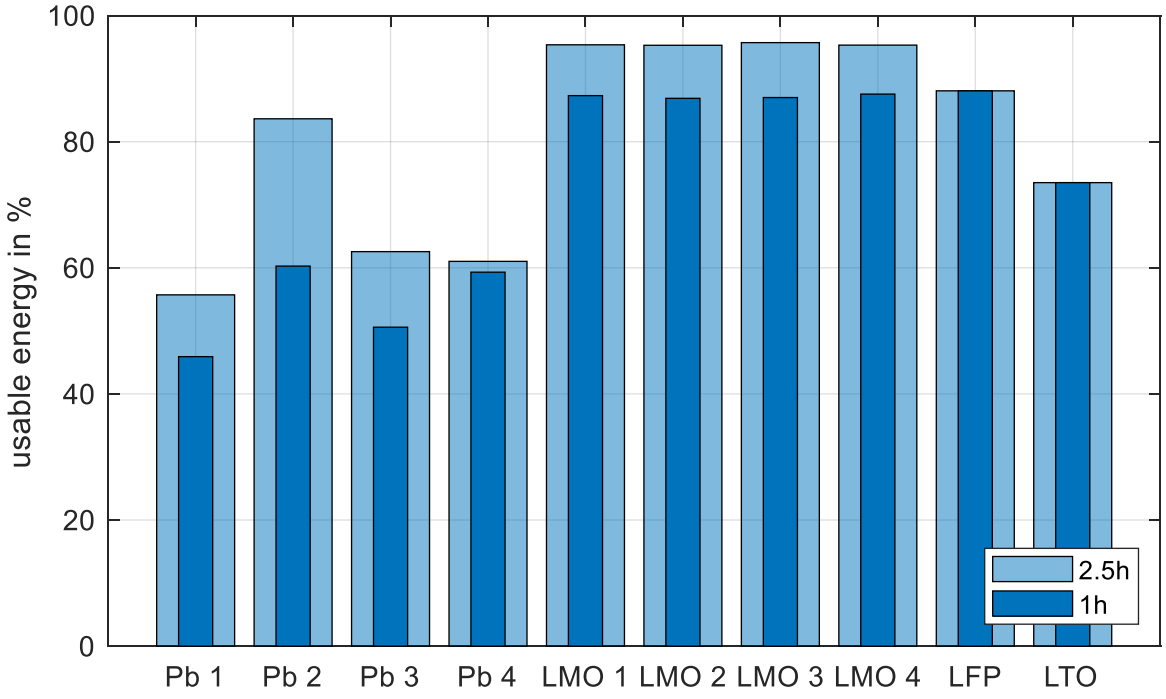

Figure 10: Usable energy (discharging process) for each battery unit according to the test in relation to the nominal energy shown in Table 1. Due to lower discharging rates the energy for 1/3 C according to Table 1 is used to calculate the shown values for all lead-acid batteries while for the Li-ion batteries the 1 C energy was taken. Due to the lack of proper balancing the LFP and LTO battery units' values are lower than the actual SOH.

The measured energy values for charging and discharging for all battery units on AC and DC side can be found in the appendix.

3.2.4 LMO 1 example

Using the LMO 1 battery unit as an example, characteristic charge and discharge curves are presented in Figure 11. The LMO 1 battery unit was chosen as an example for several reasons. LMO batteries have been used in the past and are currently still used in BESS. In addition, the performance curves are comparable and transferable to other Li-ion batteries. Finally, the LMO battery units were almost permanently loaded with the maximum possible power during the test, which also clearly shows the behavior in the marginal range. In Figure 11 on the left y-axis power and current are plotted, while the battery unit voltage is plotted to the right y-axis.

The testing procedure always started with a constant power discharge followed by a constant voltage discharge. Then a break and the constant power charge and constant voltage charge process follow. The constant power charging or discharging events a characterized by the lines parallel to the x-axis. Since the AC power was specified as the setpoint, it always corresponds to 630 kW. For the discharging process, the DC power is slightly higher than the AC power and for the charging process the DC power is slightly lower than the AC power. These differences occur due to losses within the inverter. In the constant power discharging phase, the current constantly increases while the voltage constantly decreases. In the charging phase, the opposite happens and the current constantly decreases while the voltage increases.

In the constant voltage phases, the battery voltage is kept constant at the end of charge / discharge voltage until the current falls below a certain limit. In Figure 11 can be observed that in the constant voltage phase the current and power decrease in an exponential way until the charging or discharging process is finished.

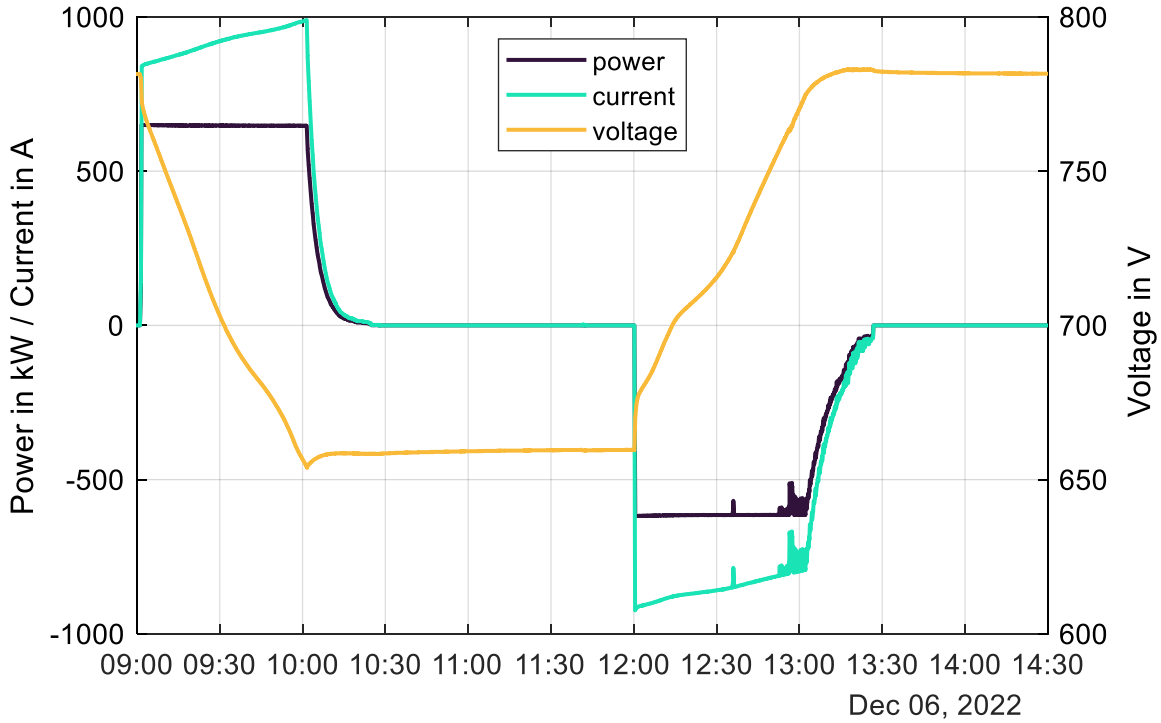

Figure 11: DC charging and discharging curves for battery unit LMO 1

For using lithium-ion batteries in marketable applications, it is recommended only to use the battery units in a SOC range where the exponential course of the power output or current is not touched. In this way battery limits become not critical in marketing operations.

3.2.5 Li-Ion cell voltage differences

In this section the cell voltages are discussed and the cell voltage differences give insights in the quality and state of balancing. In Figure 12 all LMO battery units are shown while the results for the LFP and LTO battery unit are presented in Figure 13. In the figures the lowest and highest cell voltage is shown. The SOC curve is only presented for the LFP and LTO battery unit and helps to find the constant power and constant voltage phases and makes the unusable part of the capacity clearer. Next to the figures, the mean and maximum cell voltage differences for all li-ion battery units is listed in Table 4.

The LMO battery units perform very similar to each other. The minimum and maximum cell voltages curves overlap in large portions of the graph. In a low SOC the cell voltage difference is with around 100 mV larger than in all other SOCs. This makes the lowest percentage points of the SOC unusable. Overall, the LMO battery units have cell voltage differences of around 50 mV.

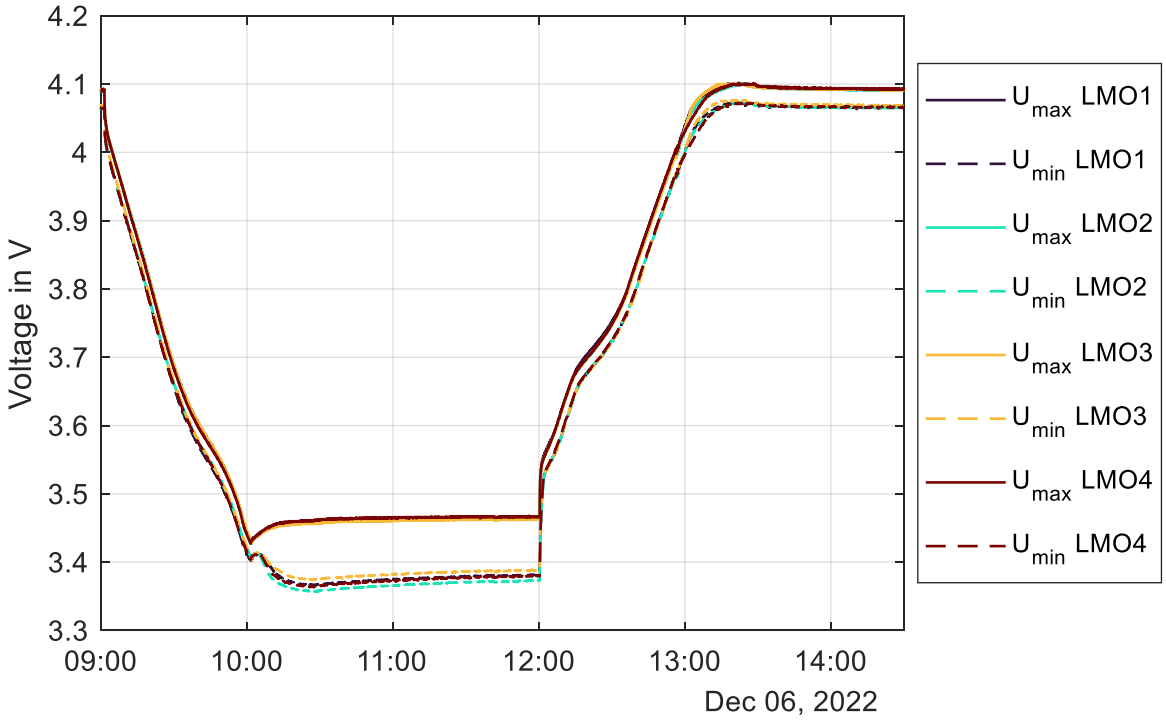

Figure 12: SOC and cell voltages for LMO battery units

The cell voltage differences of the LFP and LTO battery units are significantly larger than those of the LMO battery unit, from which it can be deduced that the cell balancing of the

LFP and LTO battery units is poorly implemented. Despite a flatter open circuit voltage curve for the LFP battery unit the average voltage difference is 91 mV and the largest difference is 294 mV. This high imbalance makes balancing necessary and makes a large portion of the capacity unusable. After the alternating charging power and thus alternating voltages around 13:00 to 13:30 the LFP battery unit started a balancing process. From 13:30 the cell voltage difference becomes significant smaller than before.

For the LTO battery unit no such balancing process is visible despite even higher cell voltage differences. The average voltage difference is with 167 mV the highest for all li-ion battery units and the maximum cell voltage difference of 529 mV is a hint to very different cell SOCs within the battery unit. A proper balancing algorithm should prevent such high voltage differences. For this battery unit it means that the balancing is not working correctly or is not implemented correctly. For the use of those battery units a significant portion of the nominal energy is not usable. Next to the energy, the power output at the boundary regions of the SOC is reduced.

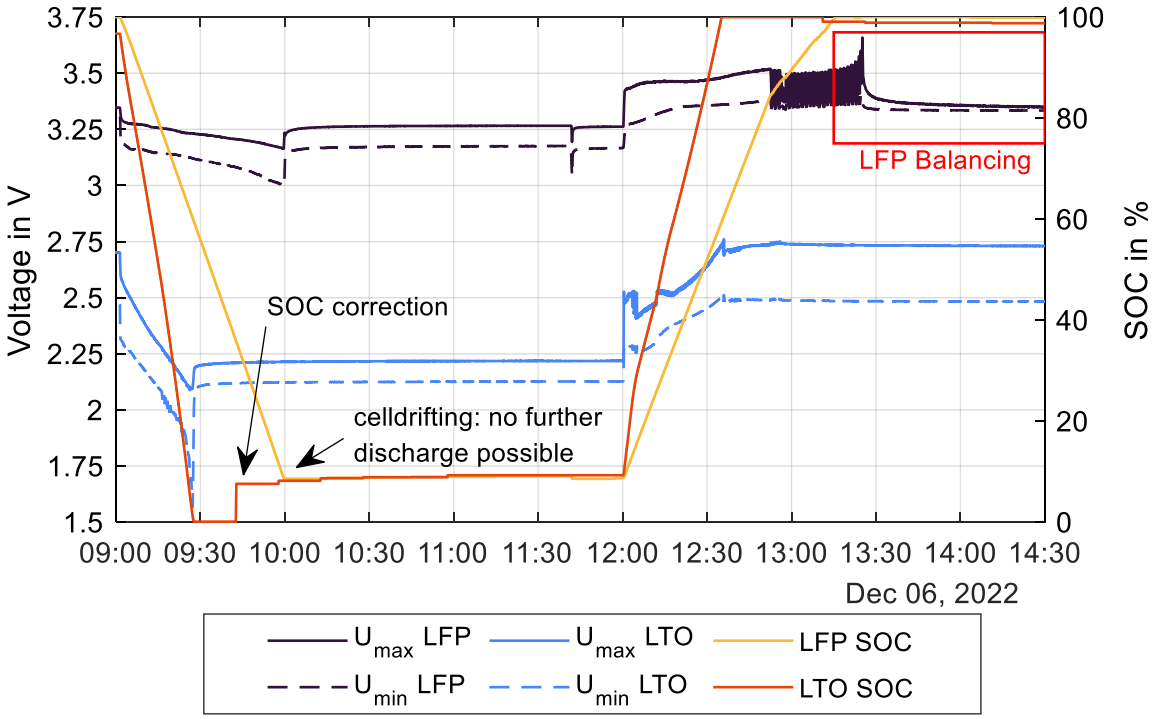

Figure 13: SOC and cell voltages for LFP and LTO battery units

Table 4: Mean and maximum cell voltage difference for all li-ion battery units measured within the testing process

Battery Unit	Mean cell voltage difference in mV	Maximum cell voltage difference in mV
LMO1	49	94
LMO2	50.52	102
LMO3	43.32	85
LMO4	49.38	98
LFP	91.39	294
LTO	166.94	529

Due to the shown spread of cell voltages of Li-ion batteries and the previously shown performance limitations in high and low SOC ranges, not all SOC regions are equally suitable for reliable and stable operation.

3.3 Recommended operational windows

From all pervious results, from testing and operational experience is not recommended to use the full 100 % SOC range for daily use. All battery units behave different and in border areas of the SOC the battery units are limited in the capabilities.

Therefore in Figure 14 all results are shown in simplified way. Note that all results and recommendations only apply directly to the M5BAT BESS but can also be used as an indicator for other BESS.

The LTO battery unit provides full power in large parts (10 – 90 %) of the SOC window. Due to challenging balancing and to protect against low state of charge, the LFP battery unit should only be used in the SOC window of 20 – 80 % and can safely deliver full power there. The LMO battery units can deliver full power in discharge direction up to 10 % SOC, but in charge direction only up to 80 % SOC. From there on, the power must be reduced due to high cell voltages.

The lead-acid batteries can only be used with limited power in large parts of the SOC. Full power is available in the discharge direction from 100 % to approximately 50 % SOC, while in the charge direction the full charge power is only available from 0 to 50 % SOC.

In reference to the BESS M5BAT, 5 MW are available in the SOC range from 30 to 70 %. In an extended SOC range from 20 to 80 %, only about 4MW are available and in the upper and lower 10 %, only a power of less than 1 MW is possible.

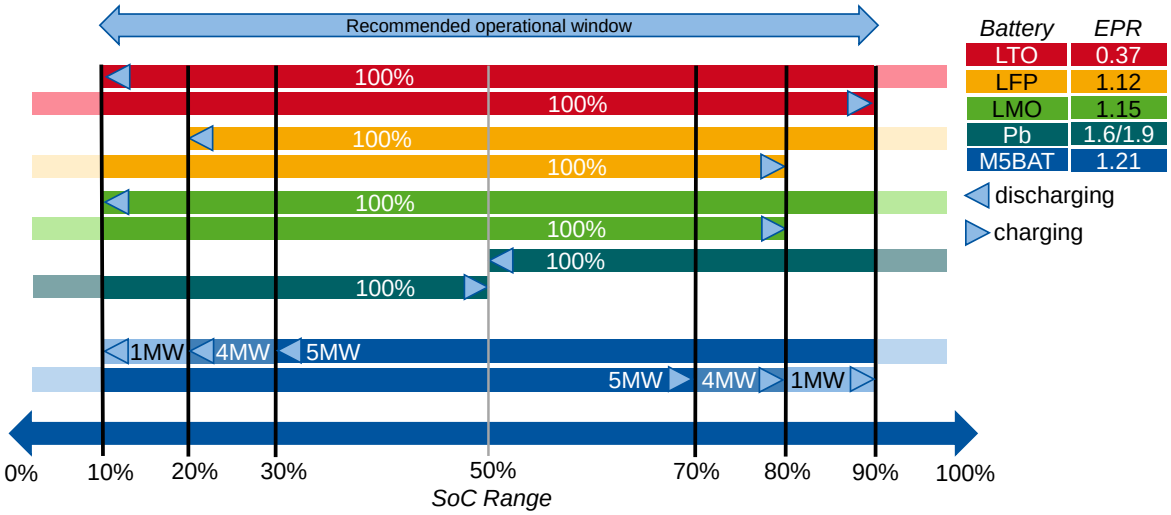

Figure 14: From operational experience and testing recommended operational windows for the battery units used in M5BAT and the whole BESS M5BAT. EPR according to 1 C values in Table 1.

3.4 Usage example

In order to illustrate the results as generally as possible, in the following we provide an example graphic for discharging a battery storage unit in relation to the currently available products on the market. Figure 15 shows the available battery power over time for a lithium-based BESS for different power outputs. The example BESS has an EPR of around 1 and is fully charged at time 0 min. The red shaded box in Figure 15 represents a 15 min market product while the green box represents a 1 h product.

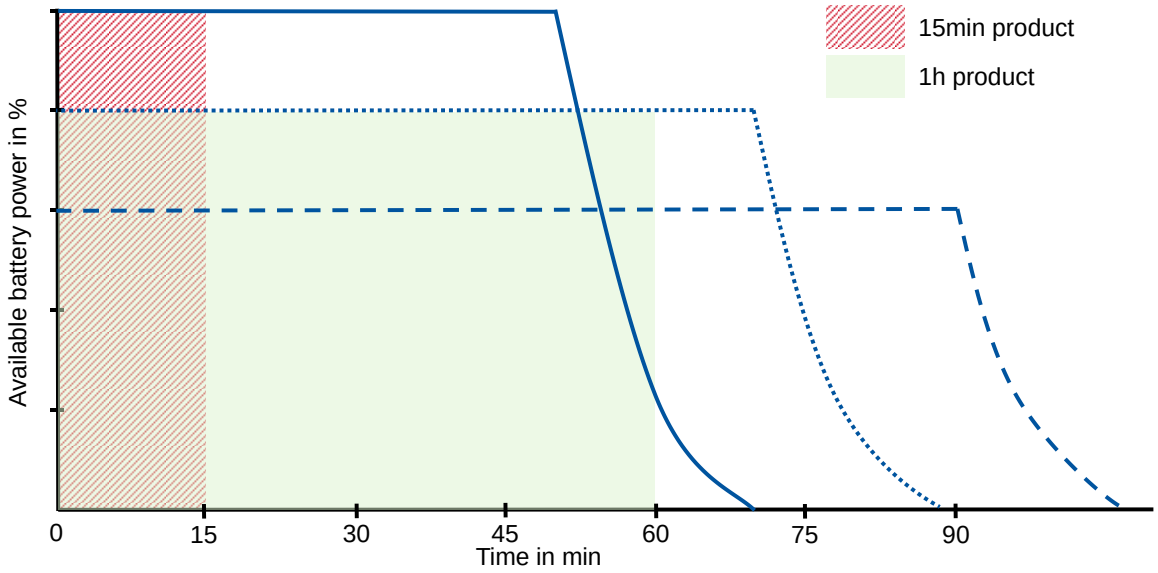

Figure 15: Schematic power curves for discharging of BESS with an EPR of ~1. Lines represent available power over time while the shaded red and green boxes represent durations of market products.

It becomes clear that a 15 min market product can easily be served with full battery power output. The 15 min product can also be served multiple times with full power output. For 1 h products the BESS design with an EPR of 1, adjustments in the power output have to be made. Just from calculations the BESS contains enough energy to serve a 1 h product. But the available power is not constant over the full SOC and discharge time which leads to the conclusion that a 1 h product cannot be served with this BESS at fully power. At reduced power the 1 h product can on contrary be served. With even more reduced power the 1 h product and additional 15 min products can be served.

The knowledge of the available power over time and over SOC are crucial for marketing activities. By reducing the usable SOC window like recommended in Figure 14 the BESS stays in a safe window where the full power can be served all the time.

4 Conclusion and outlook

It can be stated that it is extremely important to know the characteristic power curves of the BESS well for any marketing activities. The performance curves are mainly dependent on the battery technology and differ dramatically. In this study, the "best" performance curves were shown for lithium-ion batteries over a wide range of the SOC.

Furthermore, the current condition of the battery storage must be considered. Due to battery aging, a part of the capacity is lost and thus a part of the marketable power and energy. In addition to battery aging, however, the status of the balancing and thus the usable capacity is also of enormous importance. Even if the energy and capacity are available, they may not be usable due to unfavorable conditions of the individual battery cells. Hence, a monitoring and power prediction system is necessary for marketing activities.

We showed that for the M5BAT BESS the usable energy of the lithium-ion battery units varies between 75 % and 90 % while the lead-acid batteries offer only around 60 % usable energy. Moreover, the lithium-ion battery units at M5BAT have a constant power output between 10 % and 80 % SOC, while the lead-acid batteries can be discharged with full power until 50 % SOC and can be charged up to 50 % with full power. If the lead-acid batteries are not at 50 % a lower power output has to be accepted.

The issues shown with battery balancing and battery aging must be continuous monitored to ensure safe and reliable operation. Especially older BESS or second life batteries should implement a monitoring system.

5 Acknowledgements

The research was supported by the German Federal Ministry of Economic Affairs and Climate Action (BMWK) and by the project partner Uniper SE as part of the public project M5BAT (Funding Code: 03ESP265F) and EMMUseBat (Funding Code: 03EI4034).

6 Author contributions

Lucas Koltermann: Conceptualization, Methodology, Software, Validation, Formal Analysis, Investigation, Data Curation, Visualization, Writing - Original Draft

Mauricio Celi Cortés: Conceptualization, Validation, Writing - Review & Editing

Jan Figgener: Conceptualization, Validation, Writing - Review & Editing, Supervision

Sebastian Zurmühlen: Validation, Writing - Review & Editing, Project administration, Funding acquisition

Dirk Uwe Sauer: Validation, Resources, Writing - Review & Editing, Supervision, Funding acquisition

7 References

[1] J. Figgener *et al.,* “The development of stationary battery storage systems in Germany – A market review,” *Journal of Energy Storage*, vol. 29, p. 101153, 2020, doi: 10.1016/j.est.2019.101153.

[2] J. Figgener *et al.,* “The development of stationary battery storage systems in Germany – status 2020,” *Journal of Energy Storage*, vol. 33, p. 101982, 2021, doi: 10.1016/j.est.2020.101982.

[3] J. Figgener *et al.,* “The development of battery storage systems in Germany: A market review (status 2022),” 2022, doi: 10.48550/arXiv.2203.06762.

[4] Sandia National Laboratories, *DOE Global Energy Storage Database.* [Online]. Available: https://www.energystorageexchange.org/projects/data_visualization/ (accessed: Jan. 27 2023).

[5] X. Luo, J. Wang, M. Dooner, and J. Clarke, “Overview of current development in electrical energy storage technologies and the application potential in power system operation,” *Applied Energy*, vol. 137, pp. 511–536, 2015, doi: 10.1016/j.apenergy.2014.09.081.

[6] F. Wankmüller, P. R. Thimmapuram, K. G. Gallagher, and A. Botterud, “Impact of battery degradation on energy arbitrage revenue of grid-level energy storage,” *Journal of Energy Storage*, vol. 10, pp. 56–66, 2017, doi: 10.1016/j.est.2016.12.004.

[7] S. Lamp and M. Samano, “Large-scale battery storage, short-term market outcomes, and arbitrage,” *Energy Economics*, vol. 107, p. 105786, 2022, doi: 10.1016/j.eneco.2021.105786.

[8] X. Zhang, C. Qin, E. Loth, Y. Xu, X. Zhou, and H. Chen, “Arbitrage analysis for different energy storage technologies and strategies,” *Energy Reports*, vol. 7, pp. 8198–8206, 2021, doi: 10.1016/j.egyr.2021.09.009.

[9] R. L. Fares and M. E. Webber, “What are the tradeoffs between battery energy storage cycle life and calendar life in the energy arbitrage application?,” *Journal of Energy Storage*, vol. 16, pp. 37–45, 2018, doi: 10.1016/j.est.2018.01.002.

[10] E. Abramova and D. Bunn, “Optimal Daily Trading of Battery Operations Using Arbitrage Spreads,” *Energies*, vol. 14, no. 16, p. 4931, 2021, doi: 10.3390/en14164931.

[11] S. Englberger, A. Jossen, and H. Hesse, “Unlocking the Potential of Battery Storage with the Dynamic Stacking of Multiple Applications,” *Cell Reports Physical Science*, vol. 1, no. 11, p. 100238, 2020, doi: 10.1016/j.xcrp.2020.100238.

[12] C. Zhang, J. Qiu, Y. Yang, and J. Zhao, “Trading-oriented battery energy storage planning for distribution market,” *International Journal of Electrical Power & Energy Systems*, vol. 129, p. 106848, 2021, doi: 10.1016/j.ijepes.2021.106848.

[13] J. M. Reniers, G. Mulder, and D. A. Howey, “Unlocking extra value from grid batteries using advanced models,” *Journal of Power Sources*, vol. 487, p. 229355, 2021, doi: 10.1016/j.jpowsour.2020.229355.

[14] P. Kubiak, Z. Cen, C. M. López, and I. Belharouak, “Calendar aging of a 250 kW/500 kWh Li-ion battery deployed for the grid storage application,” *Journal of Power Sources*, vol. 372, pp. 16–23, 2017, doi: 10.1016/j.jpowsour.2017.10.063.

[15] M. Swierczynski, D.-I. Stroe, A.-I. Stan, R. Teodorescu, R. Laerke, and P. C. Kjaer, “Field tests experience from 1.6MW/400kWh Li-ion battery energy storage system providing primary frequency regulation service,” in *IEEE PES ISGT Europe 2013*, Lyngby, Denmark, Oct. 2013 - Oct. 2013, pp. 1–5.

[16] M. Koller, T. Borsche, A. Ulbig, and G. Andersson, “Review of grid applications with the Zurich 1MW battery energy storage system,” *Electric Power Systems Research*, vol. 120, pp. 128–135, 2015, doi: 10.1016/j.epsr.2014.06.023.

[17] M. Dubarry, A. Devie, K. Stein, M. Tun, M. Matsuura, and R. Rocheleau, “Battery Energy Storage System battery durability and reliability under electric utility grid operations: Analysis of 3 years of real usage,” *Journal of Power Sources*, vol. 338, pp. 65–73, 2017, doi: 10.1016/j.jpowsour.2016.11.034.

[18] G. Baure, A. Devie, and M. Dubarry, “Battery Durability and Reliability under Electric Utility Grid Operations: Path Dependence of Battery Degradation,” *J. Electrochem. Soc.*, vol. 166, no. 10, A1991-A2001, 2019, doi: 10.1149/2.0971910jes.

[19] G. Baure and M. Dubarry, “Battery durability and reliability under electric utility grid operations: 20-year forecast under different grid applications,” *Journal of Energy Storage*, vol. 29, p. 101391, 2020, doi: 10.1016/j.est.2020.101391.

[20] M. Dubarry and A. Devie, “Battery durability and reliability under electric utility grid operations: Representative usage aging and calendar aging,” *Journal of Energy Storage*, vol. 18, pp. 185–195, 2018, doi: 10.1016/j.est.2018.04.004.

[21] M. Dubarry, M. Tun, G. Baure, M. Matsuura, and R. E. Rocheleau, “Battery Durability and Reliability under Electric Utility Grid Operations: Analysis of On-Site Reference Tests,” *Electronics*, vol. 10, no. 13, p. 1593, 2021, doi: 10.3390/electronics10131593.

[22] J. M. Reniers and D. A. Howey, “Digital twin of a MWh-scale grid battery system for efficiency and degradation analysis,” *Applied Energy*, vol. 336, p. 120774, 2023, doi: 10.1016/j.apenergy.2023.120774.

[23] B. Wu, W. D. Widanage, S. Yang, and X. Liu, “Battery digital twins: Perspectives on the fusion of models, data and artificial intelligence for smart battery management systems,” *Energy and AI*, vol. 1, p. 100016, 2020, doi: 10.1016/j.egyai.2020.100016.

[24] D. J. Rogers, L. J. Aslett, and M. C. Troffaes, “Modelling of modular battery systems under cell capacity variation and degradation,” *Applied Energy*, vol. 283, p. 116360, 2021, doi: 10.1016/j.apenergy.2020.116360.

[25] K. Jacqué, L. Koltermann, J. Figgener, S. Zurmühlen, and D. U. Sauer, “The influence of frequency containment reserve on the cycles of a hybrid stationary large-scale storage system,” *Journal of Energy Storage*, vol. 52, p. 105040, 2022, doi: 10.1016/j.est.2022.105040.

[26] K. Jacqué, L. Koltermann, J. Figgener, S. Zurmühlen, and D. U. Sauer, “The influence of frequency containment reserve on the efficiency of a hybrid stationary large-scale storage system,” *Journal of Energy Storage*, vol. 52, p. 104961, 2022, doi: 10.1016/j.est.2022.104961.

[27] K. Jacqué, L. Koltermann, J. Figgener, S. Zurmühlen, and D. U. Sauer, “The Influence of Frequency Containment Reserve on the Operational Data and the State of Health of the Hybrid Stationary Large-Scale Storage System,” *Energies*, vol. 15, no. 4, p. 1342, 2022, doi: 10.3390/en15041342.

[28] T. Thien, H. Axelsen, M. Merten, and D. U. Sauer, “Energy management of stationary hybrid battery energy storage systems using the example of a real-world 5 MW hybrid battery storage project in Germany,” *Journal of Energy Storage*, vol. 51, p. 104257, 2022, doi: 10.1016/j.est.2022.104257.

[29] T. Thien, D. Schweer, D. vom Stein, A. Moser, and D. U. Sauer, “Real-world operating strategy and sensitivity analysis of frequency containment reserve provision with battery energy storage systems in the german market,” *Journal of Energy Storage*, vol. 13, pp. 143–163, 2017, doi: 10.1016/j.est.2017.06.012.

[30] J. Münderlein, M. Steinhoff, S. Zurmühlen, and D. U. Sauer, “Analysis and evaluation of operations strategies based on a large scale 5 MW and 5 MWh battery storage system,” *Journal of Energy Storage*, vol. 24, p. 100778, 2019, doi: 10.1016/j.est.2019.100778.

[31] Lucas Koltermann *et al.,* “Potential analysis of current battery storage systems for providing fast grid services like synthetic inertia - Case study on a 6 MW system,” *Journal of Energy Storage*, vol. 57, p. 106190, 2023, doi: 10.1016/j.est.2022.106190.

[32] Institute for Power Generation and Storage Systems (RWTH Aachen), “Modularer multi-Megawatt multi-Technologie Mittelspannungs-Batteriespeicher (M5BAT): Abschlussbericht, Datenblätter sowie weiteres Aktenarchiv,” 2018.

[33] L. Koltermann, K. Jacqué, J. Figgener, S. Zurmühlen, and D. U. Sauer, “Operational Validation of a Power Distribution Algorithm for a Modular Megawatt Battery Storage System,” *Batteries & Supercaps*, vol. 6, no. 3, 2023, doi: 10.1002/batt.202200414.

[34] D. Cittanti, A. Ferraris, A. Airale, S. Fiorot, S. Scavuzzo, and M. Carello, “Modeling Li-ion batteries for automotive application: A trade-off between accuracy and complexity,” in *2017 International Conference of Electrical and Electronic Technologies for Automotive: Turin (Italy), June 15-16, 2017*, 2017, pp. 1–8.

[35] R. Korthauer, Ed., *Lithium-ion batteries: Basics and applications*. Berlin, Heidelberg: Springer, 2018.

8 Appendix

The charged and discharged energy for each battery unit is divided into a 1 h and a 2.5 h value and differentiated between an AC value behind the inverter and a DC value for only the battery unit and presented in Figure 16. The 2.5 h values are light colored while the 1 h value is intense colored. For all battery units except the LTO battery unit the energy charged or discharged is larger for 2.5 h than for 1 h. This indicates that the LTO battery unit is loaded with an E-Rate higher than 1 E while all other battery units are loaded with lower E-rates.

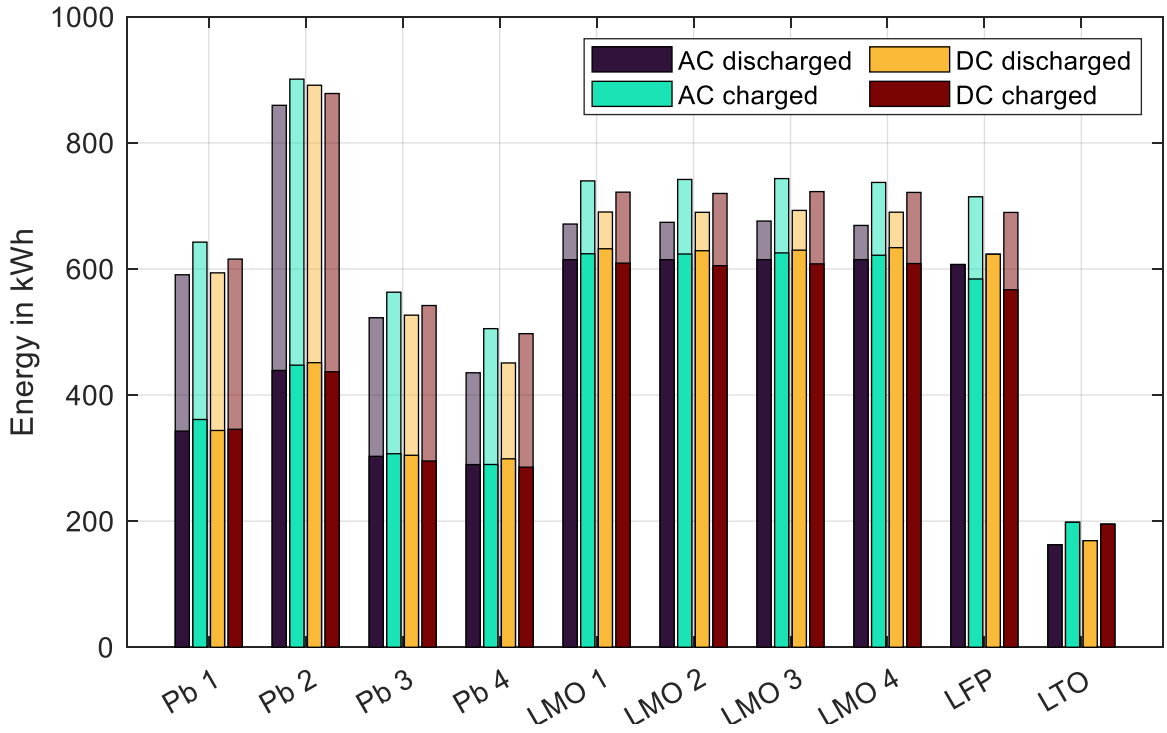

Figure 16: Energy throughput per battery unit within the test: light colors 2.5 h value; intense colors 1 h value